KITEGEN : A REVOLUTION IN WIND ENERGY GENERATION

*M. Canale, L. Fagiano, M. Milanese**

Dipartimento di Automatica e Informatica, Politecnico di Torino,

Corso Duca degli Abruzzi 24, 10129 Torino, Italy.

ABSTRACT - Control of tethered airfoils is investigated, in order to devise a new class of wind generators to overcome the main limitations of the present wind technology, based on wind mills. A model from the literature is used to simulate the dynamic of a kite whose lines are suitably pulled by a control unit. Energy is generated by a cycle composed of two phases, indicated as the traction and the drag one. The kite control unit is placed on the arm of a vertical axis rotor, connected to an electric drive able to act as generator when the kite pulls the rotor and as motor in dragging the kite against the wind. Control is obtained by "fast" implementation of Nonlinear Model Predictive Control (NMPC). In the traction phase the control is designed such that the kite pulls the rotor arm, maximizing the amount of generated energy. When energy cannot be generated anymore, the control enters the drag phase and the kite is driven to a region where the energy spent to drag the rotor is a small fraction of the energy generated in the traction phase, until a new traction phase is undertaken. Simulation results are presented, showing encouraging performances.

Keywords: emerging control applications, power systems, wind energy

1. INTRODUCTION

The solution of the problem posed by electric energy generation from fossil sources (high costs due to large demand increases in front of limited resources, pollution and CO_2 production, geopolitical use of the fossil sources by the few producer countries) is an urgent and strategic issue of our society. It is evident that these problems can be overcome only with the use of sources which are renewable, cheap, easily available and sustainable for the environment. Actual renewable technologies have not such potentials. Indeed, even the most

optimistic forecast on the diffusion of present renewable sources (wind, photovoltaic, biomasses) estimates to reach no more than 20% of contribution within the next 15-20 years. In particular, wind mills currently represent the largest component of renewables generation capacity (excluding hydro power plants) [1]. However, they require heavy towers, foundations and huge blades, which make a significant impact on the environment, require massive investments and long-term amortization periods. All these problems are reflected in electric energy production costs that are not yet competitive, in strict economic sense, with the ones of fossil energy, even considering the rise of oil and gas prices. Moreover, wind farms have problems of land occupation and environmental impact due to their generated power density per km^2, which is unacceptably lower (up to 200-300 times) than that of thermal plants. In order to overcome such limitations at Politecnico di Torino a new project has been started to design and build a new class of wind energy generators, indicated as KiteGen. The key idea (see the patents [2], [3]), which was originally investigated in [4], is to capture wind energy by means of tethered airfoils whose flight is suitably driven by an automatic control unit. Similar research projects are undergoing in several research groups and companies around the globe (for further informations, the interested reader is referred to [5]-[15]). It is expected that a wind generator of this type will have a much lower territory occupation than a wind farm of the same power (by a factor up to 50-100) and much lower electric energy production costs (by a factor up to 10-20). In the first step of the KiteGen project a small scale prototype has been realized (see Figure 1) to show the capability of controlling the flight of a single kite, by pulling the two lines which hold it, in such a way to extract a significant amount of energy. In [6] such a capability has been investigated in simulation, employing the kite model used in [16]. In particular, in the configuration considered in [6], denoted as *yo-yo* configuration, the Kite control unit (see Figure 2) has two electric drives, which act as motors

* Corresponding author. Tel. number: 0039-011.564.70.20, Fax: 0039-011.564.70.99 e-mail address: mario.milanese@polito.it

to pull the lines for controlling the flight or for recovering the kite and as generators when the line length increases due to the traction exerted by the kite. The electric actuators which hold the lines are fixed with respect to the ground. Energy is generated by continuously repeating a cycle composed of two phases: the traction and the recovery ones. In the traction phase the control is designed such that the kite pulls the lines, so that a certain amount of energy is generated. When the maximal length of the lines is reached, the control enters into the recovery phase and the kite is driven to a region where the lines can be pulled by the motors until the minimal length is reached, spending a small fraction of the energy generated in the traction phase. Configurations similar to the yo-yo have been also investigated in [7]-[11].

In this paper, an analysis of the energy generation potential of KiteGen will be presented by means of a different configuration. In particular, a *carousel* structure like the one depicted in Figure 3 is considered. In this case, several airfoils are controlled by their control units, placed on the arms of a vertical axis rotor (see Figure 3), and the control is designed to maximize the power transmitted by the airfoils to the rotor, which is connected to an electric generator. The torque opposed to the motion by the electric generator is suitably controlled in order to keep the rotation speed constant. Energy is generated by continuously repeating a cycle composed of two phases, namely the traction and the drag ones. These phases are related to the angular position Θ of the control unit, with respect to the wind direction (see Figure 4). During the traction phase, which begins at $\Theta = \Theta_3$ (see Figure 4), the control is designed in such a way that the kite pulls the rotor, maximizing the generated power. Then, when $\Theta = \Theta_0$ the drag phase begins: the kite is no longer able to generate a positive power until angle Θ reaches the value Θ_3. In this phase, the control is designed to move the kite, with as small energy loss as possible, in a suitable position to begin another traction phase. Note that the carousel configuration has been also described in [12], where a variable line length during the cycle was employed. Here, the lenght of the kite lines is kept constant during the cycle, using the

same kite and carousel parameters, and the obtained results are compared with those of [12], to evaluate the performance difference between these two operational solutions.

The control design is carried out using a Fast implementation of a Model Predictive Controller (FMPC) as proposed in [17], [18] and used also in [6], [12] for power kite control. Indeed, in each carousel phase the design is formulated as an optimization problem with its own cost function, aimed to maximize the overall generated power, with state and input constraints, since for example the kite height on the ground cannot be negative and the control actuators have their own physical limits. From this point of view, Model Predictive Control (MPC) appears to be an appropriate technique. However, a "fast" implementation is needed for the real time control computations at the required sampling time (of the order of 0.1 s). It can be noted that MPC technique has been also employed in [13] and [16] for kite control. However, in these works, the MPC controller is employed to track pre-computed kite trajectories. In this paper, no kite path is preassigned to be tracked. The obtained kite trajectory is on the contrary determined by the direct optimization of the generated energy.

2. KITE GENERATOR MODEL

In this paper, a single arm rotor generator is considered. The kite control unit is located at the end of the rotor arm, whose length is indicated with R. Rotation of the generator rotor around the fixed vertical axis Z is given by angle Θ, as depicted in Figure 4. Wind speed vector is represented as $\vec{W}_l = \vec{W}_0 + \vec{W}_t$, where $\vec{W}_0$ is the nominal wind speed, supposed to be known, which is parallel to the ground and whose magnitude $|W_0(Z)|$ is a known function, giving the wind nominal speed at a certain height Z. The term $\vec{W}_t$ may have components in all directions and is not supposed to be known, accounting for wind unmeasured turbulence. The generator rotor motion law is given by the following equation:

$$J_z \ddot{\Theta} = R F^c - T^{\text{gen}} \tag{1}$$

where J_z is the rotor moment of inertia, F^c is the tangent component, with respect to the rotor, of the pulling force exerted by the kite on its lines and T^{gen} is the torque given by the electric generator linked to the rotor. T^{gen} is positive when the kite is pulling the rotor toward increasing Θ values, thus generating energy, and it is negative when the electric generator is acting as a motor to drag the rotor between Θ_0 and Θ_3 during the drag phase, as depicted in Figure 4. A suitable local controller calculates the value of T^{gen} in order to keep a constant rotor speed $\dot{\Theta}_{\text{ref}}$. The kite dynamics are described by the model originally developed in [16]. Applying Newton's laws of motion to the kite in the local coordinate system and considering that the length of the lines is kept constant, the kite laws of motion are obtained: the considered forces acting on the kite include the contributions of gravitational force, apparent inertial force, aerodynamic force and pulling force exerted by the kite on the lines.

The aerodynamic force depends on the effective wind speed $\vec{W}_e$, which in the local system is computed as:

$$\vec{W}_e = \vec{W}_a - \vec{W}_l \tag{2}$$

where $\vec{W}_a$ is the kite speed. By considering a suitable coordinate system, the aerodynamic force can be expressed as the vector sum of the drag force F_D and of the lift force F_L, whose magnitudes are calculated as:

$$\begin{aligned} F_D &= -\frac{1}{2} C_D A \rho |W_e|^2 \\ F_L &= -\frac{1}{2} C_L A \rho |W_e|^2 \end{aligned} \tag{3}$$

where ρ is the air density, A is the kite characteristic area, C_L and C_D are the kite lift and drag coefficients. All of these variables are supposed to be constant. The lift force gives the main contribution to force F^c needed for power generation. The control variable is angle ψ

defined by

$$\psi = \arcsin\left(\frac{\Delta l}{d}\right) \tag{4}$$

with d being the distance between the two lines fixing points at the kite and Δl the length difference of the two lines. Practically, angle ψ influences the kite motion by changing the direction of the aerodynamic force vector $\vec{F}^{\text{aer}}$.

Thus the system dynamics are of the form:

$$\dot{x}(t) = g(x(t), u(t), \vec{W}_l(t)) \tag{5}$$

where $x(t) = [\theta(t)\ \phi(t)\ \Theta(t)\ \dot{\theta}(t)\ \dot{\phi}(t)\ \dot{\Theta}(t)]^T$ and $u(t) = \psi(t)$. All the model states are assumed to be measured, to be used for feedback control.

3. KITE CONTROL USING NMPC

Nonlinear Model Predictive Control or Receding Horizon Control strategy (see [19] for a survey) is widely employed in control of complex, nonlinear processes with constraints. The control move computation is performed at discrete time instants defined on the basis of a suitably chosen sampling period Δ_t. At each sampling time $t_k = k\Delta_t, k \in \mathbb{N}$, the measured values of the state $x(t_k)$ and of the nominal wind speed $W_0(t_k)$ are used to compute the control move through the optimization of a performance index of the form:

$$J(U, t_k, T_P) = \int_{t_k}^{t_k+T_P} L(\tilde{x}(\tau), \tilde{u}(\tau), W_0(\tau))d\tau \tag{6}$$

where $T_P = N_p\Delta_t, N_p \in \mathbb{N}$ is the prediction horizon, $\tilde{x}(\tau)$ is the state predicted inside the

prediction horizon according to the state equation (5), using $\tilde{x}(t_k) = x(t_k)$ and the piecewise constant control input $\tilde{u}(t)$ belonging to the sequence $U = \{\tilde{u}(t)\}, t \in [t_k, t_k + T_P]$ defined as:

$$\tilde{u}(t) = \begin{cases} \bar{u}_i, \forall t \in [t_i, t_{i+1}], i = k, \ldots, k + T_C - 1 \\ \bar{u}_{k+T_c-1}, \forall t \in [t_i, t_{i+1}], i = k + T_C, \ldots, k + T_P - 1 \end{cases} \quad (7)$$

where $T_C = N_C \Delta_t, N_C \in \square, N_C \leq N_P$. The function $L(\cdot)$ in (6) is suitably defined on the basis of the performances to be achieved in the operating phase which the kite generator lies in. Moreover, in order to take into account physical limitations on both the kite behaviour and the control input ψ, linear constraints of the form $F\tilde{x}(t) + G\tilde{u}(t) \leq H$ have been included too. Thus the predictive control law is computed using a receding horizon strategy:

1. at time instant t_k, get $x(t_k)$
2. solve the optimization problem

$$\min_U \quad J(U, t_k, T_P)$$

subject to

$$\dot{\tilde{x}} = g(\tilde{x}(t), \tilde{u}(t), W_0(t))$$
$$F\tilde{x}(t) + G\tilde{u}(t) \leq H, \forall t \in [t_k, t_k + T_P]$$

3. apply the first element of the solution sequence U of the optimization problem as the actual control action
4. repeat the whole procedure at time istant t_{k+1}

Therefore the predictive controller results to be a nonlinear static function of the variable vector $w(t) = [x(t), W_0(t), \dot{\Theta}_{ref}(t)]$:

$$u(t_k) = f(w(t_k)) \tag{8}$$

The value of the function $f(w(t_k))$ is typically computed by solving at each sampling time t_k the considered constrained optimization problem. However, an online solution of the optimization problem at each sampling time cannot be performed for applications which require "fast" sampling frequencies (of the order of 0.1 s for KiteGen). An approach to overcome this problem is to evaluate offline a finite number of values of $f(w)$, to be used to find an approximation $\hat{f}$ of f, suitable for online implementation. In particular the FMPC approach, introduced and described in [17], [18] and also used in [6] and [12], based on Set Membership approximation techniques, is employed here to derive the approximating function $\hat{f}$.

Cost function (6) and constraints considered for KiteGen control are now described. As highlighted in the Introduction, the main goal is to generate energy by a suitable control action on the kite. In order to accomplish this aim, a two-phase cycle has been defined. The two phases are referred to as the *traction phase* and the *drag phase*. For the whole cycle to be generative, the total amount of energy produced in the first phase has to be greater than the energy spent in the second one to move the kite in a suitable position in order to begin another traction phase.

3.1. Traction phase

The aim of this phase is to obtain as much mechanical energy as possible from the wind stream. The *traction phase* begins when the rotor angular position Θ with respect to the nominal wind vector $\vec{W}_0$ is such that the kite can pull the rotor arm (see Figure 4). Thus, the following *traction phase* initial condition is considered:

$$\Theta(t) \geq \Theta_3 \tag{9}$$

Control system objective adopted in the *traction phase* is to maximize the generated energy, thus at each time instant t_k the cost function $J(U, t_k, T_P)$ is computed as the energy generated over the finite time interval $[t_k, t_k + N_p]$. During the whole phase a suitable constraint is considered to keep the kite sufficiently far from the ground, moreover, actuator physical limitations give rise to the following constraints:

$$\begin{aligned} |\psi(t)| &\leq \overline{\psi} \\ |\dot{\psi}(t)| &\leq \overline{\dot{\psi}} \end{aligned} \tag{10}$$

Such constraint are taken into account also in the *drag phase*. As a matter of fact, during the *traction phase* other technical constraints have been added to force the kite to go along "figure eight" trajectories rather than circular ones as they cause the winding of the lines. The *traction phase* ends when the rotor angle is such that the kite is no more able to pull the rotor arm:

$$\Theta(t) \geq \Theta_0 \tag{11}$$

with $\Theta_0 \leq \pi/2$ (see Figure 4). When the condition (11) is reached, the *drag phase* can start.

3.2. Drag phase

During this phase the electric generator acts as a motor to drag the rotor between angles Θ_0 and Θ_3. Meanwhile, the kite is moved in a proper position in order to start another *traction phase*. The *drag phase* has been divided into three sub-phases. Transitions between each two subsequent drag sub-phases are marked by suitable values of the rotor angle, Θ_1 and Θ_2, which are chosen in order to minimize the total energy spent during the drag phase.

In the first sub-phase, the control objective is to move the kite in a zone where effective wind

speed $\vec{W}_e$ and pulling force component in plane (X,Y) (i.e. F^c) are much lower. Once the following condition is reached:

$$\Theta \geq \Theta_1 \tag{12}$$

the first *drag phase* part ends.

In the second drag sub-phase, control objective is to change the kite angular position in plane (X,Y) toward values which are suitable to begin another *traction phase*. The second sub-phase ends when the following condition is satisfied:

$$\Theta \geq \Theta_2 \tag{13}$$

Then, the third drag sub-phase begins: control objective is designed to decrease the kite height above the ground, thus preparing the generator for the following *traction phase*. The ending conditions for the whole *drag phase* coincide with the starting conditions for the *traction phase* (9).

4. SIMULATION RESULTS

Simulations have been performed with the values of model and control parameters reported in Table 1. Table 2 contains the state values which identify each phase starting and ending conditions and the values of state and input constraints.

The magnitude of the nominal wind speed is given as:

$$|W_0(Z)| = \begin{cases} 0.04Z + 8 & if \quad Z \leq 100m \\ 0.0172(Z - 100) + 12 & if \quad Z > 100m \end{cases} \tag{14}$$

Nominal wind speed is 8 m/s at 0 m of height and grows linearly to 12 m/s at 100 m and up to 17 m/s at 300 m of height. Moreover, to test control system robustness, wind turbulence $\vec{W}_t$ is introduced, with uniformly distributed random components along the inertial axes (X,Y,Z).

The absolute value of each component of $\vec{W}_t$ ranges from 0 m/s to 3 m/s, which corresponds to 25% of the nominal wind speed at 100 m altitude. Figure 5 shows the trajectories of the kite and of the control unit during two full cycles in nominal conditions. The kite follows "figure eight" orbits in this phase, with a period of about 4 s; about 65 orbits are thus completed in a single traction phase. The power generated during the two cycles is reported in Figure 6: the mean value is 478 kW and the consequent generated energy is 180 MJ per cycle. It can be noted that such energy generation performance is quite close to that obtained in [12] using a variable line length (i.e. 621-kW mean power), also considering that in [12] the average line length was longer (thus intercepting stronger wind) than the 300 meters considered here. Thus, the use of variable line length during the carousel cycle can be probably avoided to obtain a simpler operating cycle without a dramatic loss of performance. Note that the use of fixed line lenght also solves any possible issues related to line friction and wear. Figure 7 depicts the behaviour of the wind effective speed magnitude $|\vec{W}_e|$ during two full cycles. It can be noted that during the *traction phase* the kite speed (200-250 km/h) is about 15 times greater than the rotor tangential speed, which is equal to 18 km / h: this is one of the main advantages of KiteGen over classical wind mills, which work with much lower effective wind speed values.

5. CONCLUSIONS

The paper has presented a study aimed to investigate the capability of controlling tethered airfoils to devise a new class of wind energy generators, able to overcome the main limitations of the present wind technology based on wind mills. A *carousel* configuration has been considered and the obtained results are very encouraging, even though they are based on simulations carried out with a kite model taken from the literature, which certainly can give only an approximate description of the involved dynamics. On the other hand, the first tests

performed on the built prototype in the basic configuration introduced in [6] show a good matching between simulations and experimental results as regards the generated power, so that a reliable estimation of the energy generation capability of KiteGen can be made. Considering that the generated power grows linearly with the kite effective area, with the cube of wind speed and with the square of the aerodynamic efficiency C_L / C_D, the 450-kW mean power obtained in this paper can increase up to 1000-MW mean power, considering a wind speed magnitude of 12 m/s, by employing about one hundred bigger kites (500 m^2 area) on a 1500-m radius carousel. Such KiteGen plant would have a territory occupation 50 times lower and cost about 30 times less than a wind farm of the same nominal power.

ACKNOWLEDGEMENTS

This work was supported by Regione Piemonte under the Project “Controllo di aquiloni di potenza per la generazione eolica di energia” and by Ministero dell'Università e della Ricerca of Italy, under the National Project “Robustness and optimization techniques for high performances control systems”.

References

[1] REN21. Renewables 2007 Global Status Report. Paris: REN21 Secretariat and Washington, DC:Worldwatch Institute, 2008. See also: http://www.ren21.net/pdf/RE2007_Global_Status_Report.pdf

[2] Ippolito M. Smart control system exploiting the characteristics of generic kites or airfoils to convert energy. European patent # 02840646. 2004.

[3] Milanese M., Ippolito M. Sistema e procedimento di controllo automatico del volo di profili alari di potenza. Patent n. TO2006A000372. 2006 (in Italian).

[4] Loyd M.L. Crosswind Kite Power. Journal of Energy 1980; 4(3):106-111.

[5] Ockels, W.J. Laddermill, a novel concept to exploit the energy in the airspace. Aircraft design 2001; 4: 81-97.

[6] Canale M., Fagiano L., Ippolito M. and Milanese M. Control of tethered airfoils for a new class of wind energy generator. In: 45th IEEE Conference on Decision and Control. San Diego (CA), USA, 2006. p. 4020-4026

[7] B. Lansdorp and W.J. Ockels. Comparison of concepts for high-altitude wind energy generation with ground based generator. In: The 2nd China International Renewable Energy Equipment & Technology Exhibition and Conference. Beijing, China, 2005.

[8] B. Lansdorp, B. Remes, and W.J. Ockels. Design and testing of a remotely controlled surfkite for the Laddermill. In: World Wind Energy Conference. Melbourne, Australia, 2005.

[9] B. Lansdorp and P. Williams. The Laddermill - Innovative Wind Energy from High Altitudes in Holland and Australia. In: Windpower 06. Adelaide, Australia, 2006.

[10] B. Houska and M. Diehl. Optimal Control of Towing Kites. In 45th IEEE Conference on Decision and Control. San Diego (CA), USA, 2006. p. 2693-2697.

[11] B. Houska and M. Diehl. Optimal Control for Power Generating Kites. In: European Control Conference, Kos, Greece, 2007. p. 3560-3567

[12] Canale M., Fagiano L. and Milanese M. Power Kites for Energy Generation. IEEE Control Systems Magazine 2007; 27(6): 25-38.

[13] Ilzhöfer A., Houska B., and Diehl M. Nonlinear MPC of kites under varying wind conditions for a new class of large scale wind power generators. International Journal of Robust and Nonlinear Control 2007; 17(17): 1590-1599.

[14] Makani Power, Inc. See also: http://www.makanipower.com

[15] SkySails GmbH & Co. See also: http://www.skysails.info/english/

[16] Diehl M. Real-Time Optimization for Large Scale Nonlinear Processes. PhD thesis, University of Heidelberg, Germany, 2001.
See also: http://www.iwr.uni-heidelberg.de/~Moritz.Diehl/DISSERTATION/index.html

[17] Canale M., Fagiano L. and Milanese M. Set Membership approximation theory for fast implementation of Model Predictive Control laws. Automatica; to appear.

[18] Canale M., Fagiano L. and Milanese M. Fast Nonlinear Model Predictive Control Using Set Membership Approximation. In: 17th IFAC World Congress, Seoul, Korea, 2008. p. 12165-12170

[19] Mayne D. Q., Rawlings J. B., Rao C. V. and Scokaert P. O. M. Constrained model predictive control: Stability and optimality. Automatica 2004; 36: 789-814.

[20] Milanese M. and Novara C. Set membership identification of nonlinear systems. Automatica 2004; 40: 957-975.

[21] Milanese M., Novara C. and Pivano L. Structured Experimental Modelling of Complex Nonlinear Systems. In: 42nd IEEE Conference on Decision and Control, Maui, Hawaii, 2003. p 5538-5543

Figure captions

Figure 1. KiteGen small scale prototype

Figure 2. KiteGen control unit

Figure 3. Carousel configuration of KiteGen

Figure 4. Carousel configuration phases

Figure 5. Kite (thin line) and control unit trajectory with nominal conditions:*traction phase* (solid) and *drag phase* (dot-dash)

Figure 6. Instant (solid) and mean (dashed) power generated during two cycles, nominal conditions

Figure 7. Effective wind speed magnitude $|\vec{W}_e|$, nominal conditions

Figure 1. KiteGen small scale prototype

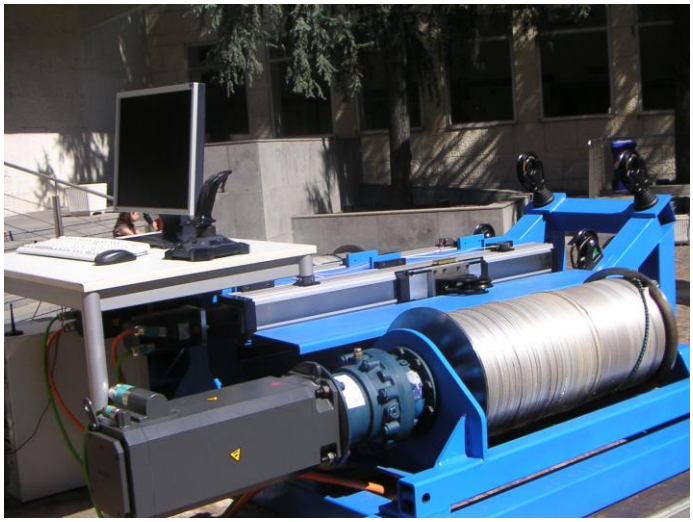

Figure 2. KiteGen control unit

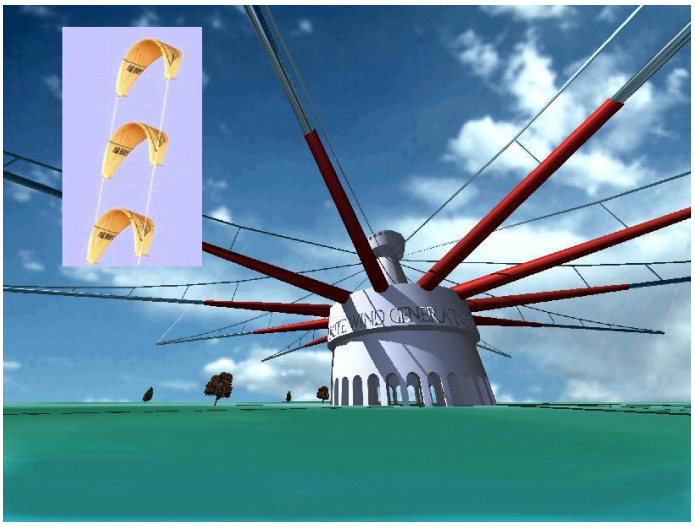

Figure 3. Carousel configuration of KiteGen

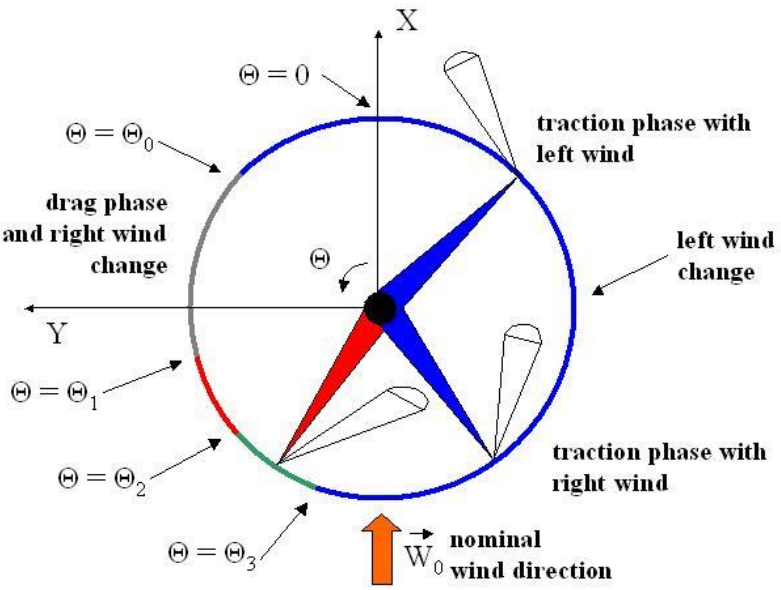

Figure 4. Carousel configuration phases

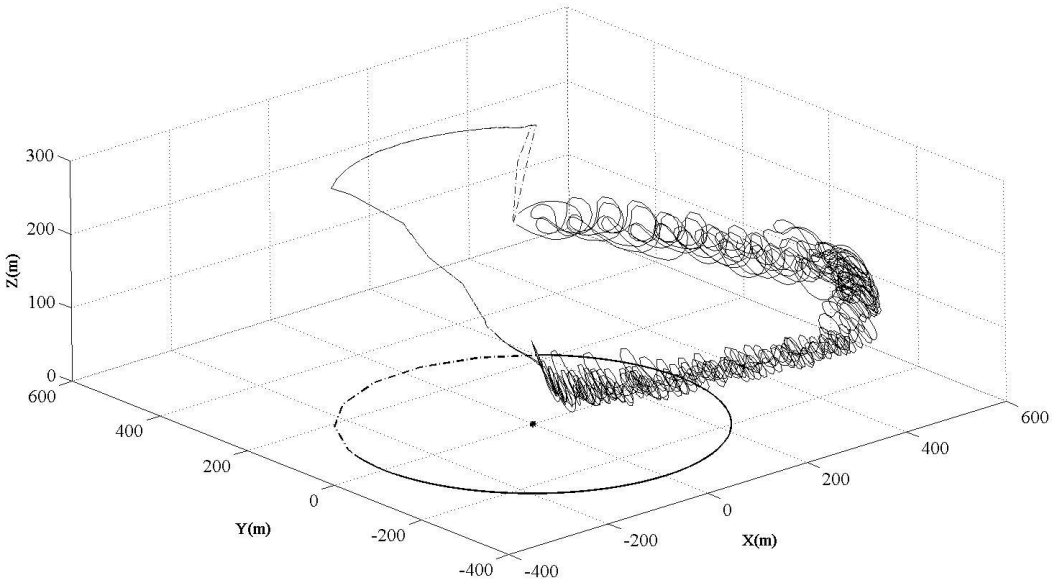

Figure 5. Kite (thin line) and control unit trajectory with nominal conditions:*traction phase* (solid) and *drag phase* (dot-dash)

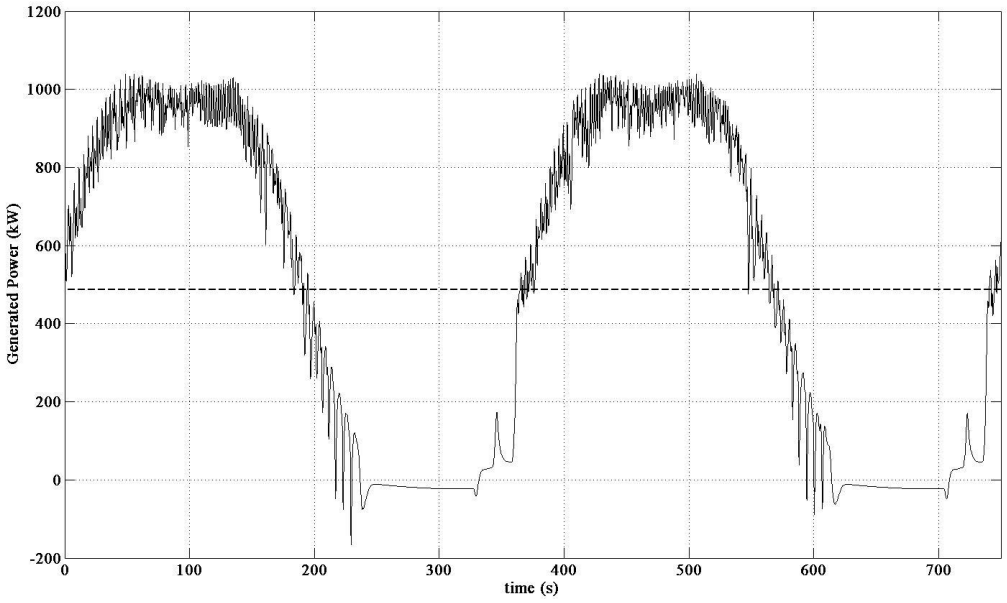

Figure 6. Instant (solid) and mean (dashed) power generated during two cycles, nominal conditions

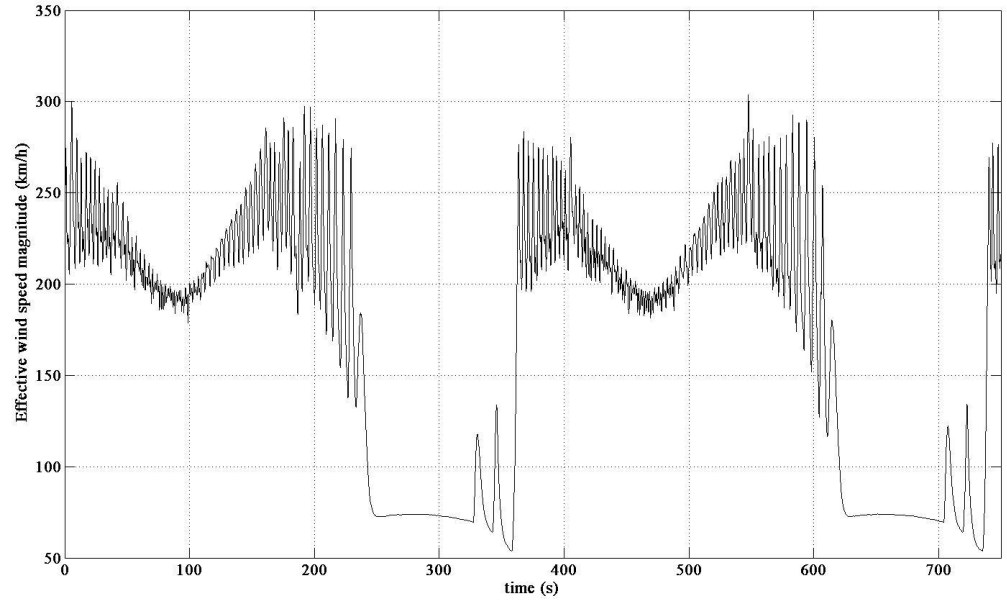

Figure 7. Effective wind speed magnitude $|\vec{W}_e|$, nominal conditions

Table 1: Model and control parameters

m	50	kite mass (kg)	C_L	1.2	lift coefficient
A	100	characteristic area (m^2)	C_D	0.15	drag coefficient
r_0	300	line length (m)	$\dot{\Theta}_{ref}$	0.16	reference $\dot{\Theta}$ (rad/s)
J_z	$9\ 10^8$	rotor moment of inertia (kg/ m^2)	T_C	0.2	sample time (s)
R	300	rotor radius (m)	N_C	1	control horizon (steps)
ρ	1.2	air density (kg/ m^3)	N_P	8	prediction horizon (steps)

Table 2: Cycle phases objectives and starting conditions, state and input constraints

Θ_0	45°	*Drag phase* starting condition	ϑ_{II}	50°	3rd Drag sub-phase objective
ϑ_I	20°	1st Drag sub-phase objective	Θ_3	165°	*Traction phase* starting condition
Θ_1	135°	2nd Drag sub-phase starting condition	$\overline{\vartheta}$	85°	State constraint
φ_I	140°	2nd Drag sub-phase objective	$\overline{\psi}$	3°	Input constraint
Θ_2	150°	3rd Drag sub-phase starting condition	$\overline{\dot{\psi}}$	20 °/s	Input constraint